Acta Pharmaceutica Sinica B 2026;16(8):5439−5451

Chinese Pharmaceutical Association
Institute of Materia Medica, Chinese Academy of Medical Sciences

Acta Pharmaceutica Sinica B

www.elsevier.com/locate/apsb
www.sciencedirect.com

ORIGINAL ARTICLE

Mussel-inspired biphasic microneedle patch for long-acting hypothyroidism treatment

Wen Zhang[a,†], Hanqing Liu[b,†], Jinxuan Hou[c,†], Kai Lei[a], Jiapeng Lei[a], Yinli Jin[a], Chuang Chen[b,*], Jianying Huang[a,*], Wei Li[a,d,e,*]

[a]*Clinical Trial Center of Zhongnan Hospital, School of Pharmaceutical Sciences, Wuhan University, Wuhan 430071, China*
[b]*Department of Breast and Thyroid Surgery, Renmin Hospital of Wuhan University, Wuhan 430060, China*
[c]*Department of Thyroid and Breast Surgery, Zhongnan Hospital of Wuhan University, Wuhan 430071, China*
[d]*TaiKang Center for Life and Medical Sciences, Wuhan University, Wuhan 430071, China*
[e]*Hubei Provincial Key Laboratory of Developmentally Originated Disease, Wuhan 430071, China*

Received 22 September 2025; received in revised form 4 April 2026; accepted 7 April 2026

KEY WORDS

Microneedle;
Long-acting;
Hypothyroidism treatment;
Sustained release;
Bioadhesive hydrogel;
Levothyroxine sodium;
Biphasic;
Transdermal drug delivery

Abstract Hypothyroidism, caused by insufficient thyroid hormone production or impaired responsiveness, is typically managed with lifelong daily oral levothyroxine sodium (LT_4). However, oral administration often suffers from variable gastrointestinal absorption and poor adherence. Here, we report a mussel-inspired biphasic microneedle (MN) patch integrating LT_4 microcrystals and a bioadhesive PDA-PAM hydrogel backing for sustained and patient-friendly hypothyroidism management. The biphasic MNs, composed of rapidly dissolving PVA/sucrose tips and a robust polystyrene base, efficiently deposit LT_4 microcrystals intradermally upon insertion, enabling gradual dissolution and sustained release. The hydrogel backing offered strong and flexible adhesion, ensuring reliable skin attachment during movement. *In vitro*, the patches exhibited first-order LT_4 release for 9 days. In hypothyroid rats, a single patch application maintained therapeutic plasma LT_4 concentrations for ∼6 days, with bioavailability comparable to intravenous injection. In a preliminary study in healthy volunteers (n = 13), placebo MN patches demonstrated high insertion efficiency, good short-term tolerability, and favorable user acceptability. While further studies are required to establish long-term safety and efficacy in patients with hypothyroidism, these findings support the feasibility of a minimally invasive, extended-interval LT_4 delivery strategy.

*Corresponding authors
E-mail addresses: chenc2469@whu.edu.cn (Chuang Chen), huangjianying@znhospital.cn (Jianying Huang), weili.mn@whu.edu.cn (Wei Li).
†These authors made equal contributions to this work.
Peer review under the responsibility of Chinese Pharmaceutical Association and Institute of Materia Medica, Chinese Academy of Medical Sciences.

https://doi.org/10.1016/j.apsb.2026.04.012

1. Introduction

Hypothyroidism is a clinical condition characterized by reduced synthesis, secretion, or inadequate biological effects of thyroid hormones[1]. It is a common disorder affecting the thyroid gland, commonly occurring in patients following thyroidectomy or with autoimmune thyroid diseases. It has been reported that the worldwide prevalence of such condition ranges from 6% to 17% in the general population[2,3]. When the functionality of the thyroid diminishes, individuals generally experience a deficiency of thyroid hormones that are essential for regulating various physiological processes and normal development[4,5], thereby leading to a range of symptoms such as compensatory hypertrophy of the thyroid, slowed metabolism, weight gain, muscular spasms, fatigue, depression, and exhaustion[1]. Therefore, it is of utmost importance to provide proactive and effective treatments for patients with hypothyroidism[6−8].

Thyroid replacement therapy is the primary treatment for hypothyroidism, aiming to correct abnormal biochemical parameters, alleviate associated symptoms and manifestations, and replenish deficient thyroid hormones in the body[5]. Levothyroxine sodium (LT_4) is the recommended lifelong substitute treatment option for all patients with persistent hypothyroidism[9]. Currently, there are various commercial oral formulations available for LT_4, including tablets and soft gel capsules[10]. Although the oral formulations provide great convenience for patients to administer the drug, these formulations still face some drawbacks. First, children and infants with hypothyroidism often have underdeveloped swallowing skills, thereby having difficulties in taking the oral tablets or capsules. Additionally, the oral administration route requires the medication to pass through the gastrointestinal tract before entering the bloodstream, which not only affects drug bioavailability due to a significant first-pass effect and rapid hepatic metabolism, but also renders LT_4 absorption susceptible to factors like gastrointestinal disorders[11,12], food intake[13,14], and concomitant medications[15,16]. Moreover, all currently marketed oral LT_4 products are all short-acting, and usually need patients with hypothyroidism to administer the drug every day for their whole life, which brings a significant challenge to patient adherence. Hence, there have been tremendous interest in developing alternative therapeutic strategies for hypothyroidism therapy that are safe, effective, age-appropriate, and capable of providing sustained drug release to enhance patient compliance.

Various sustained-release drug delivery systems have been explored for long-acting treatment of hypothyroidism, including rectal suppositories[17], liposomes[18], subcutaneous implants[19], injectable *in situ* gels[20], and transdermal hydrogels[21]. However, these approaches either require complicated procedures or administration by healthcare providers, thereby limiting patient access, or suffer from slow and limited drug absorption due to the skin barrier of stratum corneum that prevents drug permeation, or cause much pain to patients associated with hypodermic injections, which greatly reduces patient compliance. Consequently, there remains an urgent need to develop a pharmaceutical delivery system for hypothyroidism that enables long-term therapy, promotes excellent patient adherence, supports self-administration, and provides a robust sustained-release profile.

Microneedles (MNs) are a minimally invasive transdermal delivery platform designed to bypass the limitations of conventional drug administration routes[22]. Measuring only tens to hundreds of micrometres in length, MNs painlessly puncture the skin to create transient micropores, enabling rapid and efficient delivery of therapeutics into the local tissues or systemic circulation. Advances in microfabrication have greatly expanded the potential of MN-based systems[23], which have been investigated for diverse applications including wound healing[24], cancer therapy[25], hair regeneration[26], contraception[27], psoriasis management[28], and emergency medicine[29,30]. Despite these developments, the use of MNs for sustained, long-term delivery of levothyroxine for hypothyroidism remains unexplored.

Given the above objective and challenges, we report a self-administered long-acting MN patch for sustained release of the LT_4 drug for long-term therapy of hypothyroidism (Fig. 1). Specifically, a novel biphasic MN patch was developed, where LT_4 microcrystals (MCs) were encapsulated dissolvable MN tips made of PVA and sucrose and the base layer was fabricated from non-soluble polystyrene (PS). The design of PS base layer is capable of facilitating drug delivery efficiency of the MNs. Moreover, to increase the adhesion property of the MN patch and avoid patch falling from the skin during application, the MN patch was incorporated with mussel-inspired hydrogel backing composed of polydopamine-polyacrylamide (PDA-PAM)[31−33], which provides sufficient attaching capability to the patch while allowing easy removal after use. Upon skin insertion, MNs got rapid dissolution and the LT_4 MCs were directly delivered in the skin, which subsequently exhibited slow release of the hormone drug under the skin for achieving long-acting hypothyroidism therapy. In hypothyroid rats, a single administration of the MN patch maintained LT_4 plasma concentrations above the therapeutical threshold level for up to 6 days. Importantly, application of the MN patch in human participants confirmed high penetration and delivery efficiency, minimal pain, and strong user preference for the weekly MN patch over daily oral tablets, indicating its clinical potential for long-acting hypothyroidism management.

2. Materials and methods

2.1. Materials

Levothyroxine sodium pentahydrate (purity >98.0%) was purchased from Wuhan Xinxinjiali Biotech Co., Ltd (Wuhan, China). Acetone and ethylene glycol were purchased from Sinopharm Chemical Reagent Co., Ltd (Shanghai, China). Sucrose, sodium dihydrogen phosphate, sodium monohydrogen phosphate, and Sudan red III were purchased from Macklin (Shanghai, China). Polyvinyl alcohol (PVA, molecular weight: 9−10 kDa), Polystyrene (PS), and Tween 20 were purchased from Sigma−Aldrich Co (St. Louis, USA). Amobarbital sodium was purchased from

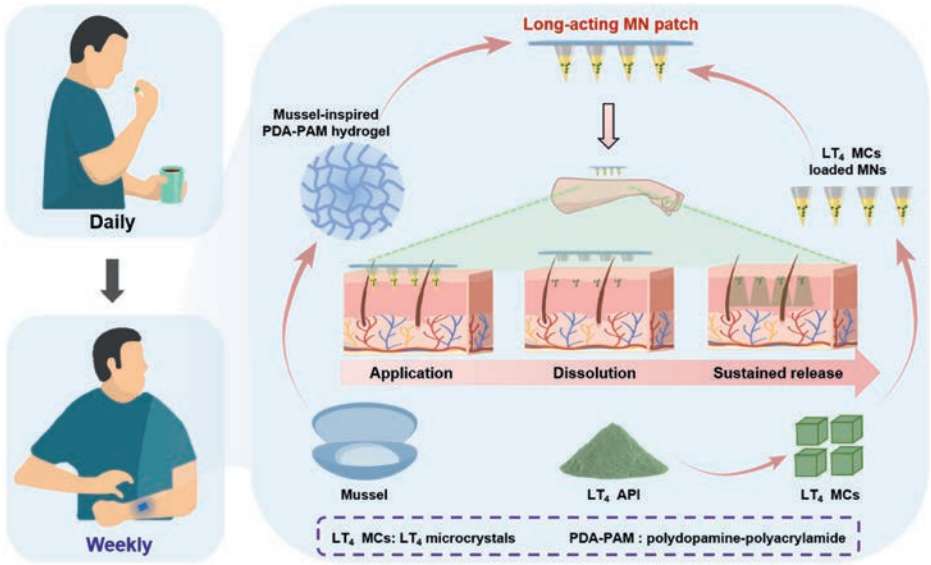

Figure 1 Schematic of mussel-inspired biphasic MN patch for long-acting hypothyroidism treatment.

Keybionet Biotechnology Co., Ltd (Nanjing, China). Hematoxylin and eosin, and 4% paraformaldehyde solution were purchased from Servicebio Co., Ltd (Wuhan, China). All of the reagents were of analytical grade. Deionized water was generated using a Milli-Q Plus 185 water purification system (Millipore).

2.2. *Preparation of LT_4 microcrystals*

The antisolvent precipitation technique was utilized to prepare LT_4 microcrystals. The organic phase consisted of a yellow solution comprising 180 mg LT_4 dissolved in 1 mL ethylene glycol, and the aqueous phase was prepared by diluting 500 mg PVA in 100 mL ultrapure water to obtain a 0.5% PVA aqueous solution, which was then stored in a refrigerated environment at 4 °C before use. The microcrystal suspension was prepared by rapidly adding 1 mL of the aforementioned organic phase to 10 mL of the aqueous phase, while maintaining at 0 °C and stirring at 800 rpm for 30 min. The resulting suspension was then transferred to a centrifuge tube and centrifugated at the speed of 10,000 rpm for 5 min, leading to the formation of microcrystal precipitates. The supernatant was removed, and the microcrystals were gently redispersed in ultrapure water. This washing step was repeated three times, after which the microcrystals were pre-frozen at −80 °C for 2 h and subsequently freeze-dried for 24 h, yielding LT_4 microcrystals.

2.3. *Characterization of LT_4 microcrystals*

To examine the morphology of LT_4 microcrystals, 10 μL of an aqueous suspension was deposited onto a silicon wafer. After water evaporation, the sample was gold-coated and imaged using scanning electron microscopy (SEM; Tescan, VEGA 3 LMU). Crystal dimensions were quantified from SEM images with ImageJ software. Fourier-transform infrared (FTIR) spectra were recorded for both LT_4 microcrystals and the active pharmaceutical ingredient (API) using an FTIR spectrometer (Thermo Fisher, Nicolet iS50). Crystal structures of the LT_4 microcrystals and API were further examined by X-ray diffraction (PANalytical, X'Pert Pro).

2.4. *Preparation and characterization of PDA-PAM hydrogel*

Dopamine hydrochloride (10 mg) was dissolved in 10 mL Tris−HCl buffer (0.01 mol/L, pH 8.5) in a penicillin bottle and stirred for 5 h to induce pre-polymerization. During this process, the solution gradually changed from yellow to brown and eventually black. Under ice-bath conditions, acrylamide (2.5 g), ammonium persulfate (250 mg), and *N*,*N*′-methylene bisacrylamide (3 mg) were added and stirred for 5 min to obtain a homogenous mixture. The ice bath was then removed, and tetramethylethylenediamine (20 μL) was introduced, followed by vortexing for 30 s. After standing for 30 min, the solution solidified into a PDA-PAM hydrogel. FTIR spectroscopy (Thermo Fisher, Nicolet iS50) was used to analyze the spectra of PDA-PAM hydrogel. The adhesion performance of the PDA-PAM hydrogel was evaluated on various substrates, including paper, plastic, glass, leaf, ceramic, rubber, stainless steel, and quartz.

2.5. *Preparation and characterization of LT_4 microcrystals-loaded biphasic MN patches*

LT_4 microcrystal-loaded biphasic MN patches were fabricated through sequential casting with poly(dimethylsiloxane) (PDMS; Dow Corning, Midland, USA) molds. For the MN tips, solution A was prepared by suspending LT_4 microcrystals (10 mg) in 1 mL of 18% (*w*/*v*) PVA and 18% (*w*/*v*) sucrose. For the backing layer, solution B was prepared by dissolving 20% (*w*/*v*) PS in dioxane.

To fabricate the patches, 50 μL of solution A was pipetted onto the PDMS mold, followed by vacuum treatment (0.1 MPa, 2 h) and centrifugation (4200 rpm, 5 min) to fill the cavities. Excess solution on the mold surface was removed. Solution B was then added to form the backing layer using the same vacuum and centrifugation steps. The molds were dried in a desiccator at room temperature (20−25 °C) for 24 h. After drying, the MN patches were integrated with PDA-PAM hydrogel, peeled from the molds, and stored in a desiccator until use. Morphology and surface composition were characterized by field-emission scanning electron microscopy (FE-SEM; Tescan MIRA) after gold sputtering. For high drug-loading MN patches, solution A contained 50 mg

LT_4 microcrystals suspended in 1 mL of 18% (*w*/*v*) PVA and 18% (*w*/*v*) sucrose.

2.6. The release of LT_4 from MN patches in vitro

Drug release from MN patches was evaluated using phosphate-buffered saline (PBS, 0.01 mol/L) containing 2% Tween 20 as the release medium. A single LT_4-loaded MN patch was sealed in a pretreated dialysis bag and placed in a conical flask on a shaker (100 rpm, 37 °C). At predetermined time points (4, 8, 12, 24 h, 2, 3, 5, 7, and 9 day), 1 mL of release medium was withdrawn and replaced with an equal volume of fresh medium to maintain sink conditions. LT_4 concentrations were quantified by UV−Vis spectrophotometry at 225 nm, and cumulative release was calculated.

2.7. Skin insertion of biphasic MN patches in vitro

The mechanical properties of MN patches were determined by a mechanical tester (Force Gauge; Mark-10). To determine the optimal application time for drug delivery, MN patches were applied to rat skin *ex vivo* for 10, 20, 30, or 40 min. At each time point, the residual MN patches were collected, and remaining LT_4 was extracted by dissolving them in 2 mL of 0.001 mol/L NaOH (pH 11) with vortexing and sonication. LT_4 content was quantified using an UV−Vis spectrophotometer, and drug delivery efficiency was calculated accordingly. To visualize skin puncture, Sudan red microcrystals, synthesized using the same protocol as LT_4 microcrystals, were loaded into the MNs instead of LT_4. The MN patch was pressed onto excised rat skin *ex vivo* for 1 min by thumb pressure and left in place for 30 min without additional force to allow complete dissolution of the tips. The patch was then removed, and puncture sites were examined under an optical microscope (Leica TL3000 Ergo). Skin samples were sectioned into 10 μm-thick frozen slices and imaged with an inverted fluorescence microscope (Olympus IX73).

2.8. Adhesion assessment biphasic MN patches

Excised rat skin was secured on a cutting board and positioned on a mechanical tester stage. MN patches attached to 3 M double-sided tape, were placed perpendicularly on the skin surface. The tester probe descended at 2.1 mm/min until a force of 1 N was reached, held for 1 min, and then retracted at 5.1 mm/min. Force changes during retraction were recorded to generate a force-displacement curve, and the maximum force during retraction was taken as the detachment force. All measurements were performed in triplicate. To evaluate material conformity to skin, PDA-PAM hydrogel or 3 M tape was applied along a digit. The digit was gradually clenched while photographs captured the hydrogel's adaptation to skin contours. For human skin testing, PDA-PAM hydrogel was applied to the forearm and removed with tweezers, with the process recorded on video.

2.9. Animals

All animal experiments were approved by the Laboratory Animal Welfare & Ethics Committee of Renmin Hospital of Wuhan university (No. WDRM20220103B). A total of 36 Wistar female rats (∼200 g) were purchased from Wuhan Bestcell Model Animal Biotech Co., Ltd. Prior to the experiments, the animals were acclimatized to the laboratory environment for 7 days. Rats were farmed with standard food and abundant space, and were kept under controlled light (12 h/12 h light/dark cycle) and temperature (20−24 °C). Rats were randomly divided into six groups, including LT_4 microcrystal-loaded MN group (75 μg/patch), blank MN group, control group without treatment, healthy group, intravenous (iv) injection group, and oral tablet group. To induce systemic hypothyroidism, total thyroidectomy was performed in rats of the LT_4 MN, blank MN, iv injection, oral tablet, and control groups following established protocols[34]. Removal of the thyroid gland inhibits endogenous thyroid hormone production, resulting in a hypothyroid state, which was confirmed when rats failed to gain weight over a 2-week period.

2.10. Application of biphasic MN patches for hypothyroidism treatment in vivo

The dorsal skin of rats was shaved prior to MN patch application. Under isoflurane anesthesia, a single LT_4 microcrystal-loaded MN patch was applied to each rat, pressed for 1 min, and left in place for 30 min. Blood samples (∼200 μL) were collected from tail veins 0, 2, 4, 6, 8, 12, 24, 48, 72 h, and 5, 7, 9, 11, and 13 days post-application. Samples were stored at 4 °C for 2 h, centrifuged at 1500×*g* for 15 min, and the serum carefully separated and stored at −80 °C. Serum LT_4 concentrations were quantified by ELISA (Ket0007, Abbkine Scientific) according to the manufacturer's instructions. All data were retained for analysis, with no outliers excluded.

To assess biocompatibility, 20 rats were sacrificed by CO_2 asphyxiation on Day 13. Four healthy control rats were maintained to evaluate skin recovery and histology following MN patch application. Major organs (heart, liver, spleen, lung, kidney) were collected, fixed in 10% neutral-buffered formalin for 24 h at 4 °C, dehydrated, embedded in paraffin, sectioned at 5 μm, and stained with hematoxylin and eosin (H&E). Blood samples collected on Day 13 were also analyzed for standard hematological parameters.

Pharmacokinetic parameters were derived using non-compartmental analysis of plasma concentrations with PKSolver (v2.0, Excel add-in) assuming extravascular input. Parameters included the first-order terminal elimination rate constant (λ_z), terminal half-life ($t_{1/2}$), time to maximum concentration (T_{max}), maximum concentration (C_{max}), area under the curve from dosing to last measurable concentration ($AUC_{0\text{-}t}$), and AUC extrapolated to infinity ($AUC_{0-\infty}$). The formula was used to calculate bioavailability (F):

$$F\,(\%) = (AUC_{0\text{-}\infty,\,MNs}/dose_{MNs})/(AUC_{0-\infty,\,IV}/dose_{IV}) \times 100 \quad (1)$$

2.11. Application, safety and acceptability of MN patches in human participants

Volunteers were excluded based on the following criteria: (1) presence of open wounds or dermatological conditions at the intended application site; (2) history of consciousness disorders or psychiatric illnesses impairing self-assessment capabilities; (3) previous allergic reactions to topical patches; (4) participation in another clinical trial within three months prior to screening; (5) pregnancy, lactation, or plans for pregnancy within three months; (6) inability to write or verbally articulate subjective sensations and thoughts clearly; or (7) any acute or chronic disease that could compromise study outcomes. Thirteen participants (19 to 30 years old) were recruited from students and staff at Wuhan University.

This study was approved by the Clinical Trial Center of Zhongnan Hospital, Wuhan University. All participants provided written informed consent prior to enrollment. The safety and acceptability of blank biphasic MN patches were evaluated on the dorsal region of the hands of healthy volunteers. Patches were applied and pressed against the skin for 1 min, followed by attaching to skin for 30 min. Patches were then removed, with the process recorded by video and puncture sites photographed. Micropores were visualized by staining the puncture sites with crystal violet for 3 min, followed by removal of excess dye with 75% ethanol swabs. The number of stained micropores was counted and compared with the total number of MNs to calculate penetration efficiency. Residual MN tips were examined under a stereomicroscope, and their heights were measured relative to original MN heights to determine delivery efficiency. Imaging was repeated at 1 and 24 h post-application. Finally, participants completed questionnaires and interviews to provide feedback on user experience, adverse reactions (*e.g.*, erythema), convenience, and preference compared with oral administration.

2.12. Statistical analysis

The experimental results are expressed as means ± standard deviation (SD). Statistical analysis was performed using a two-sided Student's *t*-test or ANOVA. Differences were considered statistically significant if $P < 0.05$ ($^{*}P < 0.05$, $^{***}P < 0.01$, and $^{***}P < 0.001$). All statistical analysis were carried out with Prism software (PRISM 5.01 GraphPad Software).

3. Results

3.1. Preparation and characterization of LT_4 microcrystals and PDA-PAM hydrogel

By employing solvent-antisolvent method, the rod-shaped LT_4 microcrystals were obtained (Fig. 2a), with uniform particle size measuring as 3.70 ± 0.61 μm (Fig. 2b). FTIR and XRD confirmed that the structural integrity and crystal morphology of LT_4 remained unchanged following the microcrystalline preparation process (Fig. 2c and d). To enhance adhesion, a PDA-PAM hydrogel was synthesized, exhibiting a microfibrillar architecture formed by interactions between PDA and PAM chains that yielded an interwoven three-dimensional network (Fig. 2e). FTIR spectra confirmed successful synthesis by the appearance of a characteristic C−N stretching vibration at 1280 cm^{-1}, indicative of interactions between the $C-NH_2$ groups of PAM and the −OH groups of PDA (Fig. 2f). The hydrogel displayed robust adhesion to diverse substrates, including leaf, plastic, paper, stainless steel,

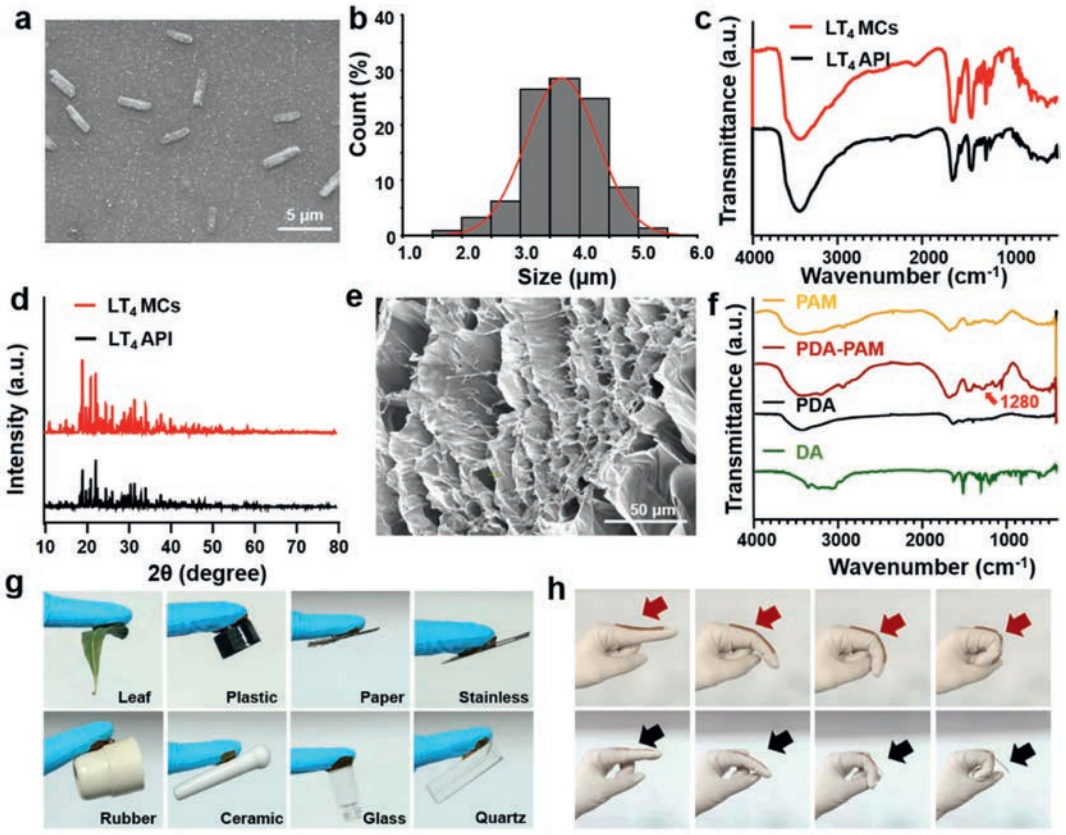

Figure 2 Characterization of LT_4 microcrystals (MCs) and PDA-PAM hydrogel. (a) SEM image of LT_4 MCs. (b) Size distribution of LT_4 MCs. (c) The FTIR spectra of LT_4 MCs and LT_4 API. (d) XRD patterns of LT_4 MCs and LT_4 API. (e) SEM of PDA-PAM hydrogel. (f) The FTIR spectra of PAM, PDA, DA, and PDA-PAM hydrogel. (g) Optical images demonstrating the adhesion of the hydrogel to various substrates. (h) Adhesion performance of the PDA-PAM hydrogel compared with 3 M double-sided tape on a human finger. The red arrowheads in the top panel indicate stable attachment of the PDA-PAM hydrogel during finger movement, whereas the black arrowheads in the bottom panel highlight detachment of the 3 M double-sided tape under the same conditions.

rubber, ceramic, glass, and quartz (Fig. 2g). Compared with commercial 3 M double-sided tape, the PDA-PAM hydrogel showed superior conformity to dynamic skin movements, maintaining stable attachment during finger bending, while being easily removed from skin without leaving residues (Fig. 2h; Supporting Video S1). These results highlight the potential of PDA-PAM hydrogel as a flexible and skin-compatible adhesive interface.

Supplementary video related to this article can be found at https://doi.org/10.1016/j.apsb.2026.04.012

3.2. Preparation and characterization of LT_4 microcrystal-loaded biphasic MN patches

To facilitate transdermal delivery, LT_4 microcrystals were incorporated into biphasic MNs consisting of a dissolvable tip layer and a water-insoluble base, integrated with a PDA-PAM hydrogel backing (Fig. 3a and b). The tip layer, composed of PVA and sucrose, provided rapid dissolution and sufficient mechanical strength, while the PS base prevented dissolution and concentrated drug loading at the needle tips, thereby enhancing transdermal delivery efficiency. Notably, solvent evaporation from the MN tips during drying was not hindered by the presence of the PS base, as the intrinsic gas permeability of the PDMS mold facilitates efficient vapor diffusion. The resulting MN patch displayed uniform geometry, with each needle measuring ~850 μm in height and ~400 μm in base diameter (Fig. 3d). Drug loading was consistent, with each MN patch containing ~75 μg of LT_4 microcrystals. Fluorescence imaging confirmed the biphasic architecture, with rhodamine B localized in the tips (red) and FITC-labelled PS in the base (green) (Fig. 3c). Elemental mapping further validated the structure: oxygen-rich components (PVA, sucrose, and PDA-PAM) were confined to the tips and backing, while carbon-rich PS dominated the base (Fig. 3e). Successful LT_4 microcrystal loading was confirmed by the presence of iodine signals co-localized with oxygen from the soluble matrix in the MN tips

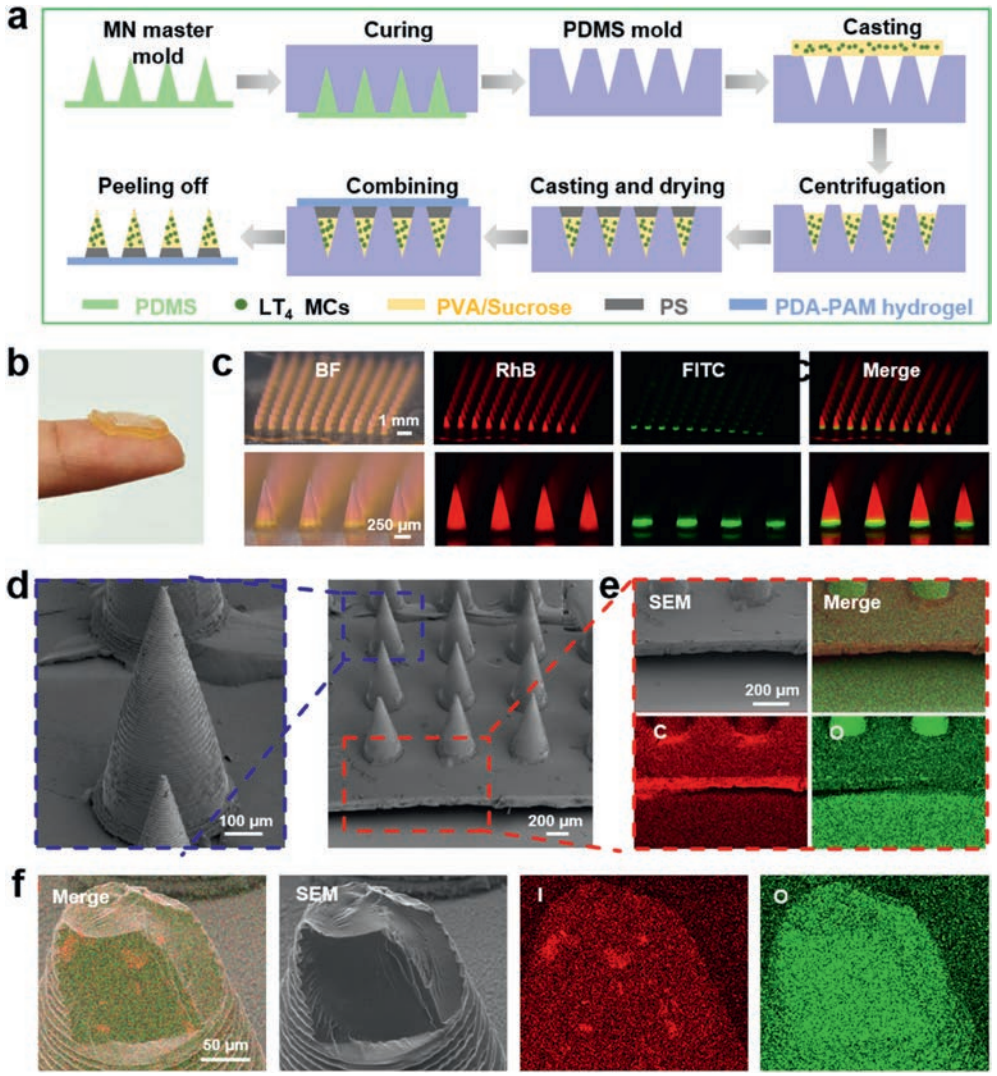

Figure 3 Fabrication and characterization of LT_4 MCs-loaded MN patches. (a) The fabrication process of LT_4 MCs-loaded MN patches by using PDMS molds. (b) Optical image of the MN patch integrated with a PDA-PAM hydrogel backing in its hydrated, as-used state. (c) Representative bright-field and fluorescence microscopy images of a MN patch containing fluorescent dyes and a dried hydrogel backing, illustrating the biphasic structure of the MNs. (d) SEM images LT_4 MCs-loaded MN patch. (e) EDS images of LT_4 MCs-loaded MN patch. (f) EDS image of the cross-section of an LT_4 MCs-loaded MN.

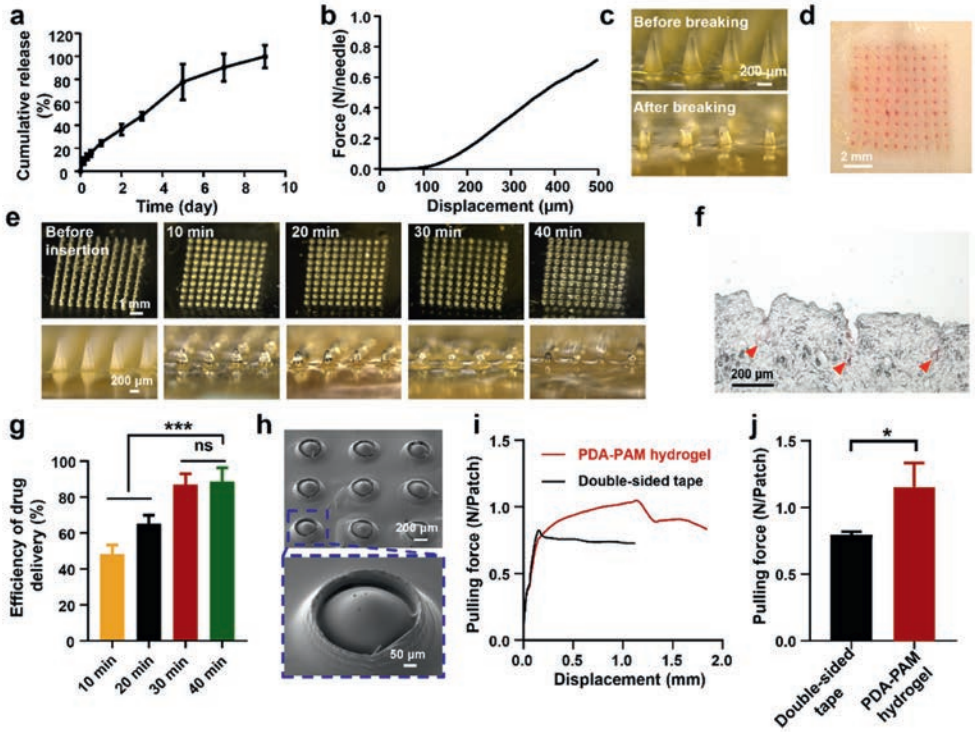

Figure 4 Application of LT_4 MCs-loaded MN patches to porcine skin *ex vivo*. (a) Cumulative LT_4 release from LT_4 MCs-loaded MN patch in PBS solution containing 2% Tween 20 at 37 °C. (b) Mechanical behavior of the LT_4 MCs-loaded hydrogel MN patch. (c) Representative optical microscopy images of the LT_4 MCs-loaded hydrogel MN patch before and after mechanical test. (d) Representative bright-field microscopy image of rat skin after Sudan red MCs-loaded MN patch insertion *ex vivo*. (e) Representative optical microscopy images of LT_4 MCs-loaded MN patches before and after insertion into the skin with different application time periods. (f) Representative image of a histological section of rat skin after Sudan red MCs-loaded MN patch insertion imaged by bright-field microscopy. Red arrowheads indicate the Sudan red MCs under skin. (g) Efficiency of drug delivery after LT_4 MCs-loaded MN patches insertion at different time points. (h) SEM images of the LT_4 MCs-loaded MN patch after dissolution for 30 min. (i) The force-displacement curve obtained in the pull-out test of skin using double-sided adhesive tape and PDA-PAM hydrogel combined with MNs (j) Maximum forces required to pull out MNs combined with double-sided adhesive tape and PDA-PAM hydrogel from skin. Each point represents mean ± SD ($n = 3$). *$P < 0.05$, ***$P < 0.001$. The ns indicates no significance.

(Fig. 3f). *In vitro* release studies in PBST (0.01 mol/L PBS, 2% Tween 20, 37 °C) demonstrated sustained, first-order LT_4 release over 9 days (Fig. 4a; Supporting information Fig. S1), indicating the long-acting potential of the MN patch for hypothyroidism treatment. Furthermore, the MN patch remained stable under light-protected conditions in a desiccator at room temperature (20−25 °C) with 20% relative humidity, exhibiting no significant changes in LT_4 loading or *in vitro* release profile (Supporting information Fig. S2). Additionally, no significant differences were observed in either drug loading or release kinetics across batches (Supporting information Fig. S3), demonstrating good inter-batch consistency and reproducibility of the MN patch formulation.

3.3. *Application of biphasic MN patch to skin ex vivo*

The biphasic MN patch exhibited sufficient mechanical strength (Fig. 4b and c; Supporting Video S2), far exceeding the 0.058 N threshold required for skin perforation[35]. To optimize application conditions, we applied the MN patch to rat skin *ex vivo* and evaluated the relationship between application time and drug delivery efficiency. As shown in Fig. 4e, dissolution of the MNs increased with application time and plateaued after 30 min, with no significant difference between 30 and 40 min (Fig. 4g). Therefore, 30 min was selected as the optimal application time for subsequent experiments.

Supplementary video related to this article can be found at https://doi.org/10.1016/j.apsb.2026.04.012

For visualization of skin insertion, MNs were loaded with Sudan red microcrystals to mimic LT_4. Before insertion, the MN patch maintained its structural integrity, with a 10 × 10 MN array and Sudan red microcrystals concentrated at the tips (Supporting information Fig. S4). Following application, the MNs dissolved almost completely (Fig. 4h), releasing the majority of Sudan red microcrystals into the skin (Fig. 4d; Supporting Video S3). Histological analysis further confirmed successful intradermal delivery of Sudan red microcrystals (Fig. 4f).

Supplementary video related to this article can be found at https://doi.org/10.1016/j.apsb.2026.04.012

To assess the contribution of PDA-PAM hydrogel to patch adhesion, MN patches were combined with either PDA-PAM hydrogel or 3 M double-sided tape, and detachment forces were measured. The PDA-PAM hydrogel-backed MN patch required an

average detachment force of 1.15 N (Fig. 4i), significantly higher than that of the double-sided tape (Fig. 4j), demonstrating the superior adhesive performance of the hydrogel backing.

3.4. Application of LT_4 microcrystal-loaded biphasic MN patch for hypothyroidism treatment in vivo

To evaluate therapeutic efficacy, the LT_4 microcrystal-loaded biphasic MN patch was applied to hypothyroid rats *in vivo*. Hypothyroidism was induced by thyroidectomy, after which body weight was monitored from Day 1 to Day 28 (Fig. 5a). Rats subjected to thyroidectomy failed to gain weight, whereas healthy rats exhibited steady weight increases (Supporting information Fig. S5), confirming successful model establishment[34]. Hypothyroid rats were randomized into five groups: (1) LT_4 microcrystal-loaded biphasic MN patch, (2) blank MN patch, (3) no treatment, (4) oral tablet, or (5) intravenous (iv) injection. Healthy rats served as negative controls. Benefiting from the strong adhesion of the PDA-PAM hydrogel, MN patches remained securely attached during rat activity and were readily removed after 30 min (Supporting information Fig. S6). MN Patches successfully penetrated rat skin, as confirmed by microscopy inspection (Fig. 5b and c) and histological analysis (Fig. 5d). Untreated hypothyroid rats and those receiving blank patches exhibited persistently low LT_4 plasma levels. In contrast, LT_4 MCs-loaded MN patch maintained therapeutic LT_4 plasma concentrations for up to 6 days[36], gradually declining to negligible levels by day 13 (Fig. 5e and f). Compared with the oral tablet, the MN patch exhibited a lower C_{max}, extended T_{max} (11.33 ± 6.77 *vs.* 6.00 ± 3.10 h), and prolonged terminal half-life (72.67 ± 42.92 *vs.* 57.27 ± 39.48 h), indicating more sustained systemic exposure. In addition, the relative bioavailability of the MN patch (72.36%) was substantially higher than that of the oral tablet (30.64%) under the tested conditions (Supporting information Tables S1 and S2). The LT_4 plasma concentration prior to dosing was used as the baseline value and was subtracted from the LT_4 plasma concentration at each time point. It is noted that the apparent discrepancy between the *in vitro* release profile (~9 days) and the *in vivo* therapeutic duration (~6 days) likely arises from physiological factors absent in the *in vitro* system, including enzymatic degradation in the skin, local blood flow, systemic clearance, and distribution into highly perfused tissues. These results demonstrate that LT_4 microcrystal-loaded biphasic MN patches achieve effective transdermal delivery and provide sustained therapeutic plasma levels, underscoring their translational potential as a long-acting treatment for hypothyroidism.

3.5. Biosafety of LT_4 microcrystal-loaded biphasic MN patch in vivo

The biosafety of the LT_4 microcrystal-loaded biphasic MN patch was systematically evaluated. Penetration sites closed completely within 15 min post-application, without visible signs of swelling or exudation (Fig. 6a), confirming the minimally invasive nature of the MN patch. H&E staining of the treated skin further revealed no significant inflammatory response compared with healthy skin.

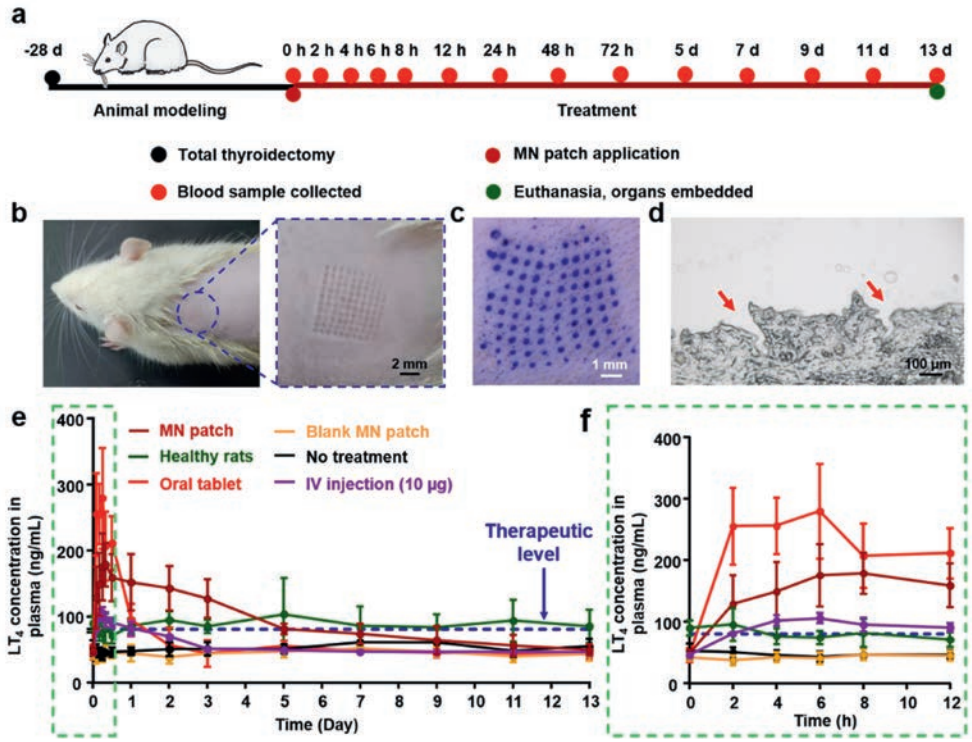

Figure 5 Performance of the LT_4 MCs-loaded MN patches in hypothyroid rats. (a) Schematic diagram of the hypothyroid rats established by total thyroidectomy and the therapeutical strategies for treatment. (b) Images of the rat skin after the insertion of one MN patch. (c) Representative image of the rat skin stained by gentian violet after MN patch insertion. (d) Bright-field microscopy image of a representative histological section of rat skin after MN patch insertion. Red arrowheads indicate micropuncture sites created by the MNs. (e) Plasma concentration of LT_4 over time following different treatments. The administered dose was 75 μg for both the MN patch and oral tablet groups, and 10 μg for the intravenous (iv) injection group. (f) Plasma concentration of LT_4 during the first 12 h post-administration. Each point represents mean ± SD (n = 6).

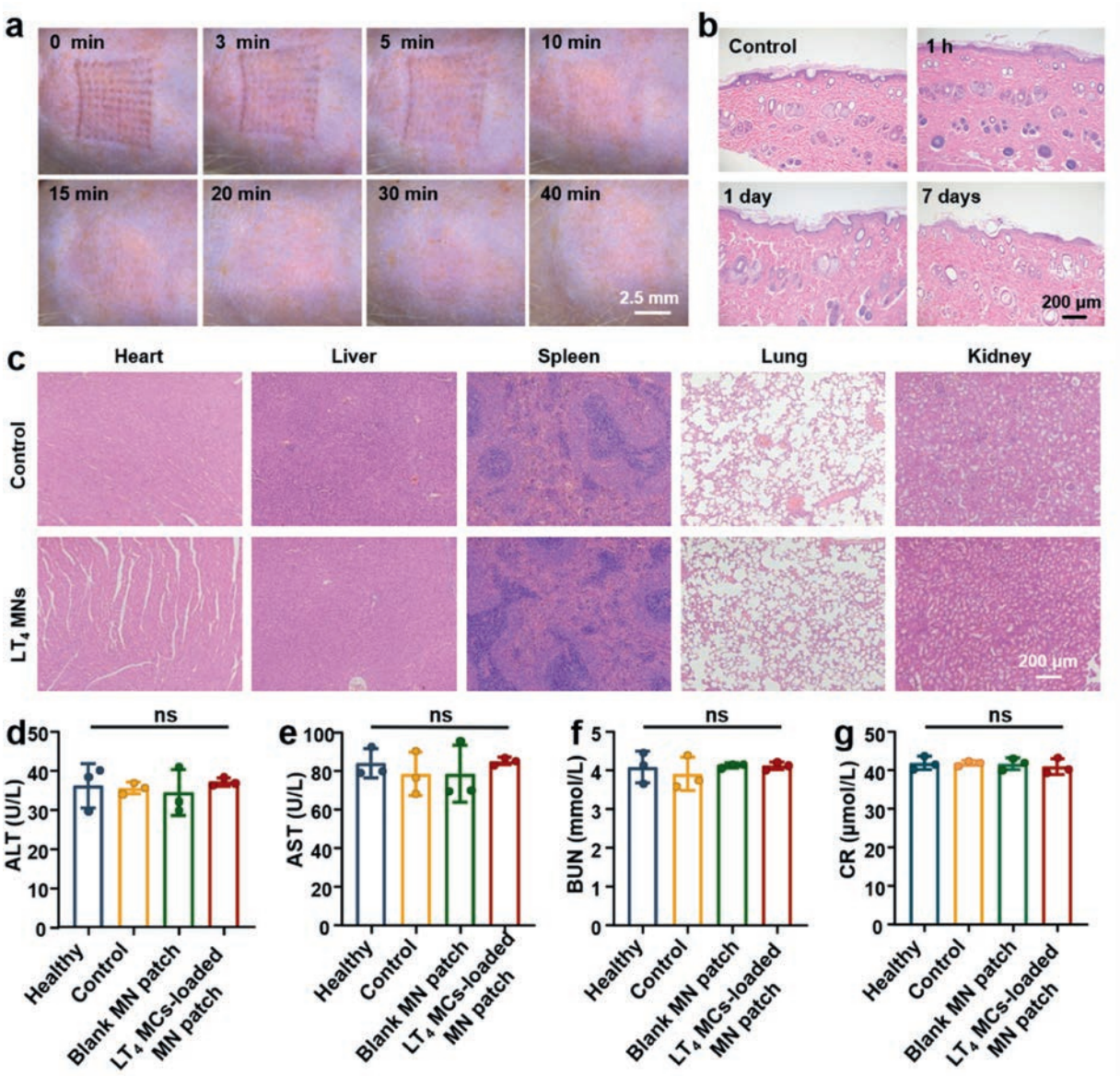

Figure 6 Biosafety and biocompatibility of the LT_4 MCs-loaded MN patches. (a) Bright-field microscopy images of rat skin recovery over time after the insertion of MN patch. (b) H&E staining images of rat skin at different time points after application of LT_4 MCs-loaded MN patches. (c) H&E staining images of heart, liver, spleen, lung, and kidney harvested from rats in healthy control and LT_4 MN patch groups on Day 13 after treatment. (d–g) Serum biochemical indicators analysis of alanine transaminase (ALT), aspartate transaminase (AST), blood urea nitrogen (BUN), and creatinine (CR) of rats after different treatments. Each point represents mean ± SD ($n = 3$). The ns indicates no significance.

Both short-term (1 h, 1 day) and long-term (7 days) observations consistently showed the absence of infection or chronic inflammation (Fig. 6b), indicating favorable skin tolerance. To evaluate systemic safety, major organs (heart, liver, spleen, lung, and kidney) from rats in MN-treated and healthy control groups were subjected to H&E staining. No appreciable histopathological abnormalities were observed in hypothyroid rats after MN patch treatment, with tissue morphology comparable to that of healthy controls (Fig. 6c). In addition, serum biochemical markers including alanine aminotransferase (ALT), aspartate aminotransferase (AST), blood urea nitrogen (BUN), and creatinine (CR) showed no significant intergroup differences (Fig. 6d), indicating preserved hepatic and renal function. Collectively, these results confirm the excellent local and systemic biocompatibility of the biphasic MN patch, supporting its safety for long-term use in hypothyroidism therapy.

3.6. Safety and acceptability of biphasic MN patches in humans

The biosafety and acceptability of the biphasic MN patch were next evaluated in healthy human participants. The patch was applied to the dorsal hand skin by pressing for 1 min, followed by a 30-min attachment without pressure before removal. As shown in Fig. 7a, the patch adhered firmly to the skin, owing to the adhesive properties of the PDA-PAM hydrogel, and could be easily removed without leaving any residue. Consistent with results in rat skin, successful skin penetration was confirmed by crystal violet staining, which revealed a well-defined 10 × 10 micropore array

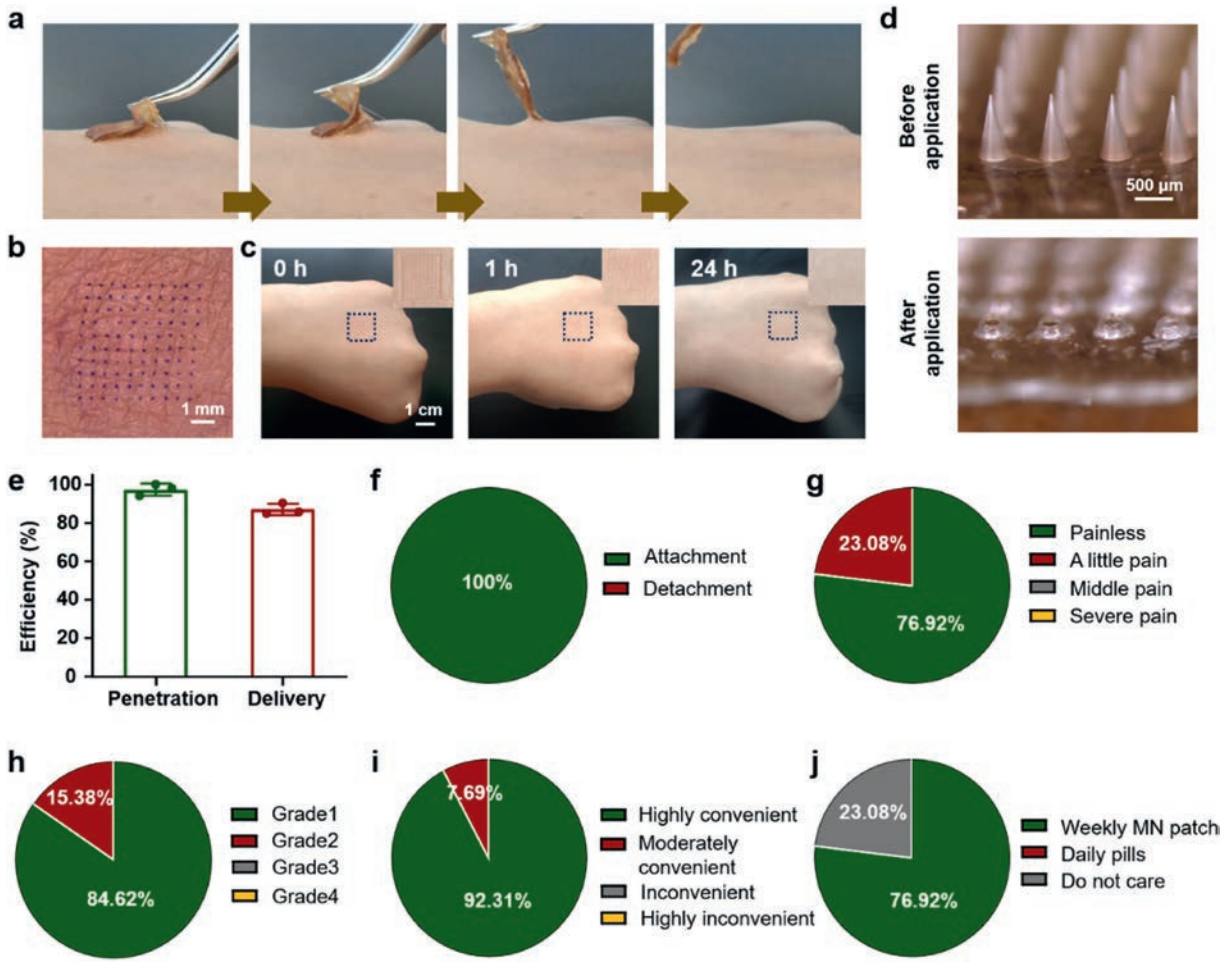

Figure 7 Application of MN patches on human participants. (a) Representative photographs of the MN patch removal process from the skin. (b) Representative photograph of skin punctured by patch after staining with gentian violet, showing successful penetration of the MNs in human skin. (c) Representative images of the skin of a human participant at different time points after application of one MN patch. The inset shows a magnified view of the application site. (d) Representative bright-field microscopy images of MNs before (top) and after (bottom) application to human skin. (e) The penetration and delivery efficiency of MN patch in human skin ($n=$ 3). (f–j) $n=$ 13 participants. (f) Attachment and detachment percentage of MN patches during application. (g) Pain feedback reported by human participants during MN patch application. (h) Erythema responses following MN patch application. (i) Participant feedback on convenience of MN patch application. (j) Participant preference for daily oral tablets versus weekly MN patch application.

at the application site (Fig. 7b). Immediately after application, faint erythema was observed, which diminished markedly within 1 h and resolved almost completely within 24 h (Fig. 7c). Examination of MNs before and after insertion showed substantial dissolution in the skin (Fig. 7d), corresponding to a penetration efficiency of 97.3% and delivery efficiency of 87.0% (Fig. 7e). All 13 participants retained the patch securely for 30 min of unrestricted movement, with no cases of detachment observed (Fig. 7f). Feedback revealed that the MN patch application was either painless (76.92%) or caused only a little pain (23.08%) (Fig. 7g), indicating the minimal invasiveness property of the MN-based formulation. Apart from transient erythema, no swelling, infection, or other adverse reactions were reported (Fig. 7h; Supporting information Table S3). Regarding usability, 92.31% of participants rated the MN patch as highly convenient, while 7.69% considered it moderately convenient (Fig. 7i). When compared with current daily oral levothyroxine therapy, 76.92% of participants expressed preference for the weekly MN patch, and 23.08% reported no preference (Fig. 7j). Collectively, these findings demonstrate that the biphasic MN patch exhibits excellent biosafety, minimal skin irritation, strong adhesion, and high user acceptability, supporting its clinical potential for long-acting hypothyroidism management.

4. Discussion

Here, we developed and validated an LT_4 microcrystal-loaded biphasic MN patch with a PDA-PAM hydrogel backing for long-acting and patient-friendly management of hypothyroidism. The biphasic MN architecture, composed of rapidly dissolving PVA/sucrose tips and a mechanically robust PS base, enabled efficient transdermal delivery of LT_4 MCs while maintaining sufficient strength for consistent skin penetration. The PDA-PAM hydrogel further provided strong, flexible adhesion and superior conformability to skin movement compared to conventional

adhesives, ensuring reliable patch attachment during use. The MN patches achieved sustained LT_4 release over 9 days *in vitro* and maintained therapeutic plasma concentrations for up to 6 days in hypothyroid rats after a single application. In vitro, the LT_4 MCs-loaded MN patches exhibited an initial release of approximately 20%−30% within the first 24 h, followed by a slower, concentration-dependent release phase. Kinetic modeling indicated that the release profile is better described by a first-order model, suggesting that LT_4 release is predominantly governed by concentration-dependent dissolution of intradermally deposited MCs followed by diffusion into surrounding tissue. *In vivo*, a transient C_{max} was observed at ∼8 h after application, likely reflecting rapid dissolution of a fraction of MCs located in well-perfused dermal regions and immediate systemic uptake. The release behavior is influenced by multiple factors, including microcrystal size and surface area, local drug concentration gradients, diffusion distance within the skin microenvironment, and total drug loading per patch. The difference between *in vitro* and *in vivo* profiles can be attributed to dynamic physiological factors, including dermal blood flow, tissue distribution, and clearance, that are not captured under static *in vitro* conditions. Despite this initial peak, therapeutic plasma LT_4 concentrations were maintained for up to 6 days, supporting sustained systemic exposure from the MN platform. Importantly, the MN patches demonstrated excellent biosafety, with rapid closure of microchannels, no local or systemic inflammation, and no adverse effects on major organs or serum biochemical markers. In a preliminary study in healthy volunteers, placebo MN patches demonstrated effective skin insertion, minimal discomfort, transient mild erythema, and favorable user acceptability. Overall, these findings highlight the feasibility of a minimally invasive, extended-interval LT_4 delivery approach, although further studies are required to establish long-term safety, optimal dosing, and therapeutic efficacy in patients with hypothyroidism.

In this study, a single LT_4 MCs-loaded MN patch (containing ∼75 μg LT_4) maintained plasma concentrations above the therapeutic threshold for ∼6 days in rats. Using standard allometric scaling from rats to humans, and considering the typical adult daily LT_4 requirement (∼50−75 μg/day), a weekly patch for humans would require a total loading of ∼450 μg LT_4. Given the high drug loading capacity of the MNs and the ability to adjust patch size or needle density, it is feasible to achieve the required therapeutic dose in a single weekly MN patch[37]. Increasing the drug load may affect MN mechanical strength, insertion efficiency, and dissolution kinetics. However, the biphasic design with a rigid PS base and dissolvable PVA/sucrose tip provides flexibility to accommodate higher drug loading without compromising skin penetration or release performance. This supports the translational potential of the system for long-acting hypothyroidism therapy in humans, while maintaining a minimally invasive and patient-friendly design. Although plasma LT_4 levels and body weight recovery were used to evaluate therapeutic response, comprehensive assessment of thyroid function ideally includes additional biomarkers such as thyroid-stimulating hormone (TSH) and T_3. Due to limitations in serum volume for serial pharmacokinetic sampling, these parameters were not measured in the present study. Therefore, the absence of TSH and T_3 data represents a limitation, and future studies will incorporate broader endocrine profiling to further confirm restoration of thyroid homeostasis.

Long-acting LT_4 delivery systems have been explored using various platforms, including subcutaneous poly(ε-caprolactone) (PCL) implants (>4 weeks)[19], injectable polymeric microspheres (>10 days)[38], and gastro-mucoadhesive systems with extended gastric residence (up to 38 days in rats)[39]. While these strategies demonstrate prolonged release durations, they typically require surgical implantation, injection by healthcare professionals, or complex gastrointestinal retention mechanisms. In contrast, the present MN platform is designed to balance sustained delivery with minimal invasiveness and practical usability. Although the ∼6-day therapeutic duration achieved here does not exceed that of implantable or injectable systems, it enables a clinically relevant weekly dosing regimen through a self-administered, transdermal format. This distinction is particularly important in hypothyroidism management, where lifelong therapy and adherence challenges remain major concerns.

Rather than maximizing duration alone, our approach emphasizes a patient-centric design that integrates sustained hormone delivery, strong bioadhesion, mechanical reliability, and demonstrated human acceptability. The combination of minimally invasive administration, secure skin attachment, and favorable user feedback positions this MN patch as a practical alternative between daily oral tablets and invasive long-acting systems. We therefore propose that the translational significance of this work lies not in achieving the longest reported duration, but in offering a clinically adaptable, self-administered weekly therapy that may improve adherence and patient experience in thyroid hormone replacement.

Although a transient peak concentration was observed following application, this effect is attributable to the rapid dissolution of a fraction of surface-exposed LT_4 MCs immediately after tip dissolution. The remaining microcrystalline depot subsequently governs sustained release through dissolution-limited kinetics. In the rat model, the observed C_{max} remained within the therapeutic range and did not induce detectable adverse effects. Nevertheless, given the narrow therapeutic index of LT_4 in clinical settings, further smoothing of the early release phase may be desirable. This could be achieved by modulating crystal size, reducing surface-associated drug fraction, or incorporating diffusion-controlling excipients within the tip matrix. Such tunability highlights the adaptability of the MN platform for clinical optimization.

It is important to note that the MN patch is designed for short-term application (∼30 min) rather than continuous wear. During this period, the MNs dissolve and deposit LT_4 MCs intradermally, which then provide sustained hormone release over several days. Consequently, the human study only assessed patch insertion efficiency, short-term tolerability, and adhesion during the application window, and did not evaluate long-term wear scenarios such as showering, sweating, or friction over multiple days. Future studies will be necessary to investigate dermatological safety and adhesion performance following repeated weekly applications, to fully support clinical translation of this patient-friendly, long-acting therapy.

Finally, the biphasic MN patch is compatible with established scalable manufacturing strategies. The fabrication process relies on micromolding and solution casting, which can be adapted to high-throughput production methods such as roll-to-roll replication or injection-molded master templates. The materials used, including PVA, sucrose, PS, and PDA-based hydrogel components, are commercially available and relatively low cost. Moreover, as a self-administered, minimally invasive system, the MN patch may reduce healthcare-associated costs compared with implantable or injectable long-acting alternatives. Although further process optimization and regulatory validation will be required, the current design does not involve rare materials or technically prohibitive steps, further supporting its feasibility for large-scale production.

Acknowledgments

This work was supported by the following fundings: National Natural Science Foundation of China (NSFC, No. 82373798, 52103182) and Thyroid research program of young and middle-aged physicians. We thank Miss Yanli Guo from the Core Facility of Wuhan University for her assistance with SEM analysis.

Author contributions

Wen Zhang: Conceptualization, Formal analysis, Investigation, Methodology, Validation, Writing original draft. Hanqing Liu: Formal analysis, Investigation, Methodology, Validation, Writing original draft. Jinxuan Hou: Methodology, Writing original draft. Kai Lei: Review & editing manuscript. Jiapeng Lei: Investigation, Methodology. Yinli Jin: Investigation, Methodology. Chuang Chen: Funding acquisition, Supervision, Review & editing manuscript. Jianying Huang: Funding acquisition, Supervision, Review & editing manuscript. Wei Li: Conceptualization, Funding acquisition, Project administration, Supervision, Validation, Review & editing manuscript.

Conflicts of interest

The authors have applied for a patent related to this study, patent application number 202311441767.3, "The preparation and application of a biphasic microneedle patch integrating the mussel-inspired hydrogel with levothyroxine sodium microcrystals for hypothyroidism treatment".

Appendix A. Supporting information

Supporting information to this article can be found online at https://doi.org/10.1016/j.apsb.2026.04.012.

References

1. Chaker L, Razvi S, Bensenor IM, Azizi F, Pearce EN, Peeters RP. Hypothyroidism. *Nat Rev Dis Primers* 2022;**8**:30.
2. Cooper DS, Biondi B. Subclinical thyroid disease. *Lancet* 2012;**379**: 1142−54.
3. Roberts CG, Ladenson PW. Hypothyroidism. *Lancet* 2004;**363**: 793−803.
4. Baksi S, Pradhan A. Thyroid hormone: sex-dependent role in nervous system regulation and disease. *Biol Sex Differ* 2021;**12**:25.
5. McDermott MT. Hypothyroidism. *Ann Intern Med* 2020;**173**:Itc1−16.
6. Garber JR, Cobin RH, Gharib H, Hennessey JV, Klein I, Mechanick JI, et al. Clinical practice guidelines for hypothyroidism in adults: cosponsored by the American association of clinical endocrinologists and the American thyroid association. *Endocr Pract* 2012;**18**:988−1028.
7. Jonklaas J, Bianco AC, Bauer AJ, Burman KD, Cappola AR, Celi FS, et al. Guidelines for the treatment of hypothyroidism: prepared by the American thyroid association task force on thyroid hormone replacement. *Thyroid* 2014;**24**:1670−751.
8. Biondi B, Wartofsky L. Treatment with thyroid hormone. *Endocr Rev* 2014;**35**:433−512.
9. Biondi B, Cooper DS. Thyroid hormone therapy for hypothyroidism. *Endocrine* 2019;**66**:18−26.
10. Colucci P, Yue CS, Ducharme M, Benvenga S. A review of the pharmacokinetics of levothyroxine for the treatment of hypothyroidism. *Eur Endocrinol* 2013;**9**:40−7.
11. d'Estève-Bonetti L, Bennet AP, Malet D, Hoff M, Louvet JP, Caron P. Gluten-induced enteropathy (coeliac disease) revealed by resistance to treatment with levothyroxine and alfacalcidol in a sixty-eight-year-old patient: a case report. *Thyroid* 2002;**12**:633−6.
12. Cellini M, Santaguida MG, Gatto I, Virili C, Del Duca SC, Brusca N, et al. Systematic appraisal of lactose intolerance as cause of increased need for oral thyroxine. *J Clin Endocrinol Metab* 2014;**99**:E1454−8.
13. Wiesner A, Gajewska D, Paśko P. Levothyroxine interactions with food and dietary supplements−a systematic review. *Pharmaceuticals (Basel)* 2021;**14**:206.
14. Chon DA, Reisman T, Weinreb JE, Hershman JM, Leung AM. Concurrent milk ingestion decreases absorption of levothyroxine. *Thyroid* 2018;**28**:454−7.
15. Centanni M, Gargano L, Canettieri G, Viceconti N, Franchi A, Delle Fave G, et al. Thyroxine in goiter, *Helicobacter pylori* infection, and chronic gastritis. *N Engl J Med* 2006;**354**:1787−95.
16. Mokrani MC, Duval F, Erb A, Gonzalez Lopera F, Danila V. Are the thyroid and adrenal system alterations linked in depression?. *Psychoneuroendocrinology* 2020;**122**:104831.
17. Hamada Y, Masuda K, Okubo M, Nakasa H, Sekine Y, Ishii I. Pharmaceutical studies of levothyroxine sodium hydrate suppository provided as a hospital preparation. *Biol Pharm Bull* 2015;**38**:625−8.
18. Rostami E, Kashanian S, Azandaryani AH. Preparation of solid lipid nanoparticles as drug carriers for levothyroxine sodium with *in vitro* drug delivery kinetic characterization. *Mol Biol Rep* 2014;**41**:3521−7.
19. Stewart SA, Domínguez-Robles J, Utomo E, Picco CJ, Corduas F, Mancuso E, et al. Poly(caprolactone)-based subcutaneous implant for sustained delivery of levothyroxine. *Int J Pharm* 2021;**607**:121011.
20. Kamali H, Khodaverdi E, Kaffash E, Saffari AS, Shiadeh SNR, Nokhodchi A, et al. Optimization and *in vitro* evaluation of injectable sustained-release of levothyroxine using PLGA-PEG-PLGA. *J Pharm Innov* 2021;**16**:688−98.
21. Bai Q, Tan J, Chai J, Shen L, Li N, Wu C. Preparation of levothyroxine transdermal gels and preliminary pharmacokinetic study in hypothyroidism rat model. *Lett Drug Des Discov* 2022;**19**:1039−48.
22. Prausnitz MR. Microneedles for transdermal drug delivery. *Adv Drug Deliv Rev* 2004;**56**:581−7.
23. Ma G, Wu C. Microneedle, bio-microneedle and bio-inspired microneedle: a review. *J Control Release* 2017;**251**:11−23.
24. Guo M, Wang Y, Gao B, He B. Shark tooth-inspired microneedle dressing for intelligent wound management. *ACS Nano* 2021;**15**:15316−27.
25. Wang C, Zeng Y, Chen KF, Lin J, Yuan Q, Jiang X, et al. A self-monitoring microneedle patch for light-controlled synergistic treatment of melanoma. *Bioact Mater* 2023;**27**:58−71.
26. Yin M, Zeng Y, Liu HQ, Zhang W, Wang C, Chen C, et al. Dissolving microneedle patch integrated with microspheres for long-acting hair regrowth therapy. *ACS Appl Mater Interfaces* 2023;**15**:17532−42.
27. Li W, Tang J, Terry RN, Li S, Brunie A, Callahan RL, et al. Long-acting reversible contraception by effervescent microneedle patch. *Sci Adv* 2019;**5**:eaaw8145.
28. Du H, Liu P, Zhu J, Lan J, Li Y, Zhang L, et al. Hyaluronic acid-based dissolving microneedle patch loaded with methotrexate for improved treatment of psoriasis. *ACS Appl Mater Interfaces* 2019;**11**:43588−98.
29. Sheng T, Jin R, Yang C, Qiu K, Wang M, Shi J, et al. Unmanned aerial vehicle mediated drug delivery for first aid. *Adv Mater* 2023;**35**: e2208648.
30. Lee J, Park S, Le PT, Lee G, Lee HW, Yun G, et al. Peripheral microneedle patch for first-aid hemostasis. *Adv Healthc Mater* 2023; **12**:e2201697.
31. Han L, Lu X, Liu K, Wang K, Fang L, Weng LT, et al. Mussel-inspired adhesive and tough hydrogel based on nanoclay confined dopamine polymerization. *ACS Nano* 2017;**11**:2561−74.
32. Han L, Yan L, Wang K, Fang L, Zhang H, Tang Y, et al. Tough, self-healable and tissue-adhesive hydrogel with tunable multifunctionality. *NPG Asia Mater* 2017;**9**:e372.
33. Han L, Lu X, Wang M, Gan D, Deng W, Wang K, et al. A mussel-inspired conductive, self-adhesive, and self-healable tough hydrogel as cell stimulators and implantable bioelectronics. *Small* 2017;**13**:1601916.
34. Bianco AC, Anderson G, Forrest D, Galton VA, Gereben B, Kim BW, et al. American Thyroid association guide to investigating thyroid

hormone economy and action in rodent and cell models. *Thyroid* 2014; **24**:88−168.
35. Lee C, Yang H, Kim S, Kim M, Kang H, Kim N, et al. Evaluation of the anti-wrinkle effect of an ascorbic acid-loaded dissolving microneedle patch via a double-blind, placebo-controlled clinical study. *Int J Cosmet Sci* 2016;**38**:375−81.
36. Kinlaw WB, Schwartz HL, Oppenheimer JH. Decreased serum triiodothyronine in starving rats is due primarily to diminished thyroidal secretion of thyroxine. *J Clin Investig* 1985;**75**:1238−41.
37. Li W, Li S, Fan X, Prausnitz MR. Microneedle patch designs to increase dose administered to human subjects. *J Control Release* 2021;**339**:350−60.
38. Alhawari HH, Abuhamdan RM, Alrashdan M, Al Thaher Y, Shraideh ZA, Abulateefeh SR. Development and *in vivo* evaluation of sustained release microparticles loaded with levothyroxine for hypothyroidism treatment. *J Pharmaceutical Science* 2024;**113**:1566−71.
39. Bollareddy SR, Chauhan SS, Venuganti VVK. Bioinspired long-acting mucoadhesive gastric patch for levothyroxine delivery. *ACS Appl Mater Interfaces* 2025;**17**:14924−39.